CrossMark

ORIGINAL CONTRIBUTION

Investigation on Dry Sliding Wear Behavior of Nylon66/GnP Nano-composite

Kota Sankara Narayana[1] · Koka Naga Sai Suman[2] · Kothapalli Arun Vikram[1]

Abstract The tribological behavior of graphene nano platelets (GnP) reinforced Nylon66 polymer Nano composites were studied using a pin-on-disc apparatus under dry sliding conditions. The influence of wear control factors like applied load, velocity, sliding distance and weight percentage of GnP reinforcement on the responses like specific wear rate and frictional coefficient were investigated. Nano composites were developed by melt mixing of various weight fractions of GnP (0/0.5/1/2) with nylon 66 using twin screw extruder. A design of experiments based on the Taguchi technique was performed to acquire data in a controlled way and was successfully used to identify the optimal combinations of control factors influencing the outputs. Analysis of variance was employed to investigate the influence and contribution of control factors on the responses. The results showed that the inclusion of GnP as reinforcing material in Nylon66 Nano composites, decreases the friction coefficient and increases the wear resistance of the Nano composites significantly.

Keywords Polymer nano composites · GnP · Taguchi · Orthogonal array · Dry sliding wear

✉ Kota Sankara Narayana
  ksn.arts@gmail.com

[1] GITAM Institute of Technology, GITAM University, Visakhapatnam 530 045, Andhra Pradesh, India

[2] AUCOE, Andhra University, Visakhapatnam 530 003, Andhra Pradesh, India

Introduction

Polymer matrix composites are of main focus for engineering applications because of their good wear resistance and low friction, high modulus of elasticity, light weight and low cost [1]. The main limitations of using polymer matrix composites are poor thermal stability, low hardness, reactive to moisture, chemicals and solvents while metal matrix composites are sensitive to acids, bases, humidity and salts which limits their applications [2]. In order to avoid these problems, glass matrix composites reinforced with carbon fibers were developed [2] and it has been a topic of research over the last three decades [3, 4]. Glass matrix composites exhibit increase in hardness, less sensitivity to moisture, acids, chemicals or salts, along with the advantage of self-lubricating effect that graphite fiber provides to the composites [5].

In recent years, work has been done on wear behavior of composites composed of various engineering polymers reinforced filler materials such as glass fiber, PTFE, zinc oxide, alumina, silica, calcium carbonate, titanium oxide, CNTS, graphite but less attention has been focused on the tribological performance of Nano composites. Due to the discovery of graphene, research studies were extended on developing graphene reinforced ceramics [6], glass matrix [7, 8], polymer matrix [9] and metal matrix composites [10]. The addition of graphene also improves the functional properties of glass/ceramic composites. Porwal et al. [7] reported that the addition of only 2.5 vol% of graphene oxide nano-platelets improves the fracture toughness of silica nano-composites by ∼35 %, when compared to pure silica glass.

Graphene consists of a two dimensional atomic layer thick sheet of carbon atoms and has better mechanical [11], electrical [12] and thermal [13] properties, when compared to graphite. Inclusion of small loading of graphene when

72

J. Inst. Eng. India Ser. D (January–June 2017) 98(1):71–78

compared to graphite, CNTs and carbon black in a matrix can lead to significant improvements in properties due to its high specific area. Fan et al. [14] reported a value of 1000 S/m electrical conductivity with addition of only 2.35 vol% of graphene nano-platelets in an alumina matrix, while Miranzo et al. [15] reported 100 % improvement in thermal conductivity of silicon nitride–graphene nano-composites. An improvement in the electrical properties of graphene nano-composites can be useful for electronic applications, while the high specific surface area and excellent mechanical properties of graphene can be useful for fabricating advanced composites with improved mechanical and tribological properties.

Graphene composites are expected to have better tribological properties compared to graphite fiber reinforced glass composites along with improved electrical and thermal properties [11–13]. Moreover, the two-dimensional platelet geometry of graphene and graphene based materials may offer certain property improvements that SWCNTs cannot provide when dispersed in polymer composites. Though a large quantum of literature is devoted to the study of sliding wear performance of synthetic as well as natural fiber composites, tribological performance of Nano composites were seldom reported. Hence in the present study, Nylon66/GnP Nano-composites with loading of different wt% of GnP were fabricated using twin screw extruder and their tribological properties were investigated using a pin on disc apparatus.

Experimentation

Materials

Nylon66 with grade 101 L was chosen as polymer matrix material, while Graphene Nano platelets (GnP) having average diameter of 5 μm, avg. thickness of 2 nm and surface area 500 m^2/g was selected as reinforcing material. Nylon66/GnP was blended in the current study and their characteristics are shown in Table 1.

Nano Composite Fabrication

Before blending, the polymer granules and fillers were dried at 80 °C for 4–5 h in a dehumidifier and then dry

filler material was hand mixed with polyamide 66 and other additives. Selected weight fraction based filler compositions were mixed with polymer and extruded in a co-rotating twin screw extruder. The L/D ratio of the screw was 40:1, main barrel speed of 200 rpm, feeder speed of 11 rpm and setting current as 16 A were maintained for all the compositions.

The extrudates from the die were quenched in a tank at 24–30 °C and then palletized. For melt blending, the temperature profile of the extrusion were Zone 1 (220 °C), Zone 2 (229 °C), Zone 3 (255 °C), Zone 4 (237 °C), Zone 5 (233 °C), Zone 6 (246 °C) Zone 7 (252 °C) with the die temperature of 239 °C and melting temperature as 243 °C. The extrudates of the composition were palletized in palletizing machine. The rpm of the palletizer was maintained in the range of 60–80 rpm. The granules of the extrudates were pre dried in dehumidifier at 80 °C for 10 h and injection molded in a microprocessor based 75 T injection molding machine fitted with a master mould containing the cavity for tensile strength, flexural and impact specimens. After its removal from the mould, specimens were sent for ageing process at room temperature for 1 or 2 days. Now the fabricated specimens were obtained as per ASTM 256 Standards. Processing parameters are Zone 1 (280 °C), Zone 2 (226 °C), Zone 3 (232 °C), Zone 4 (232 °C). The composition details of the fabricated composites with their hardness values for the present investigation are tabulated as shown in Table 2.

Friction and Wear Measurements

To evaluate the friction and sliding wear of GnP reinforced Nylon66 nano composites under dry sliding conditions, the wear tests were conducted on a pin-on-disc apparatus as

Table 2 Composition and hardness values of prepared nano composites

Material designation	Composition by wt%		Hardness (rockwell R)
	Nylon66	GnP	
PURE	100	0	110
PA66/GnP1	99.5	0.5	127
PA66/GNP2	99	1	153
PA66/GnP3	98	2	138

Table 1 Data on polymer and reinforcement

Polymer/filler	Designation	Grade	Melting point	Density	Source
Nylon66	PA66	Zytel 101L NC010	263 °C	1.14 g/cc	M/s. E.I DuPont India Pvt. Ltd.
Graphene nano platelets	GnP	GRADE C	3600 °C	2 g/cc	M/s. XG Science USA

shown in Fig. 1. The specimen was held stationary and the disc was rotated while a normal force was applied through a lever mechanism. The counter body disc is made up of hardened ground steel (EN-32, surface roughness (R_a) 0.6 μm, hardness of 72 HRC). During the test, the friction force was measured using friction monitoring unit. A personal computer-based data acquisition system was used to acquire the friction force continuously. The material loss from the composite surface is measured using a precision electronic balance with an accuracy of +0.01 mg and the average weight loss was used to calculate the specific wear rate (W_s). The difference in the weight measured before

Fig. 1 Pin-on disc apparatus

and after test gives the volume loss and the specific wear rate (mm³/Nm) is then expressed on 'volume loss' basis using Eq. (1).

$$W_s = (\Delta V/D * F_n) \tag{1}$$

where $\Delta V(mm^3)$ is loss of wear volume, D (m) is sliding distance, F_n (N) is the normal load acting on the pin.

The wear rate of the nano composites were studied as a function of the weight percentage of GnP reinforcement (wt%), sliding distance (SLD), load and velocity. Wear rate data reported here is the average of two runs.

Taguchi Design of Experiments

The Taguchi design of experiment (DOE) approach eliminates the need for repeated experiments and thus saves time, material and cost. Taguchi DOE is a powerful analysis tool for modeling and analyzing the influence of control factors on performance output. The most important stage in the design of experiment lies in the selection of the control factors. In the present work, the impact of four such control factors are studied using L_{16} orthogonal design as presented in Table 3.

Taguchi DOE based on Orthogonal Arrays (OA) generates 16 experimental runs (L_{16}) for combination of 4 factors with four levels. Taguchi L_{16} array is helpful to predict only the main effects of the control factors but not their interactions. In

Table 3 Orthogonal array L_{16} of Taguchi

Experiment no.	Main factors				Control factor				Avg. sp. wear rate W_s (*10^{-06}) (mm³/Nm)	Friction coefficient μ	SN ratio for W_s	SN ratio for μ
	A	B	C	D	A	B	C	D				
1	1	1	1	1	0	40	1	1800	0.6125	0.140	4.2578	17.0774
2	1	2	2	2	0	60	2	3600	1.0016	0.182	−0.0138	14.7986
3	1	3	3	3	0	80	3	5400	1.1518	0.240	−1.2275	12.3958
4	1	4	4	4	0	100	4	7200	1.3149	0.300	−2.3778	10.4576
5	2	1	2	3	0.5	40	2	5400	0.4261	0.116	7.4097	18.7108
6	2	2	1	4	0.5	60	1	7200	0.9852	0.150	0.1295	16.4782
7	2	3	4	1	0.5	80	4	1800	1.0173	0.180	−0.1489	14.8945
8	2	4	3	2	0.5	100	3	3600	1.2641	0.195	−2.0356	14.1993
9	3	1	3	4	1	40	3	7200	0.3311	0.096	9.6008	20.3546
10	3	2	4	3	1	60	4	5400	0.8592	0.110	1.3181	19.1721
11	3	3	1	2	1	80	1	3600	1.0059	0.128	−0.0511	17.8558
12	3	4	2	1	1	100	2	1800	1.1598	0.139	−1.2876	17.1397
13	4	1	4	2	2	40	4	3600	0.2436	0.071	7.0601	22.9748
14	4	2	3	1	2	60	3	1800	0.8896	0.121	1.0161	18.3443
15	4	3	2	4	2	80	2	7200	0.9132	0.155	0.7886	16.1934
16	4	4	1	3	2	100	1	5400	1.0095	0.140	−0.0821	17.0774

A, reinforcement (wt%); B, load (N); C, velocity (m/sec); D, sliding distance (m); W_s, average specific wear rate (mm³/Nm); μ, friction coefficient

74

J. Inst. Eng. India Ser. D (January–June 2017) 98(1):71–78

this paper, 16 runs out of 4^4 experiments were considered based on Taguchi partial factorial DOE along with recorded responses like specific wear rate (W_S) and friction coefficient (μ) as a function of four independent control factors (like load, velocity, sliding distance and wt% of reinforcement) with four levels each. The SN ratio determined using Eq. (2) are tabulated in Table 3 and are used to evaluate optimality of the control factors. Later, ANOVA is used for analyzing their influences and contribution [16, 17].

$$(SN)_{Smaller-is-Better} = -10Log\left(\frac{1}{n}\sum_{i=1}^{n}y_i^2\right) \tag{2}$$

where 'n' is observation number, 'y_i' is observation value.

The formulae for individual optimum response determination basing on the SN ratios, is mentioned in the Eq(s). (3)–(4) [18].

$$\eta_{optimum} = \eta_{avg} + \sum_{i=1}^{n}\left(\eta_{ideal} - \eta_{avg}\right) \tag{3}$$

$$Response_{optimum} = \sqrt{10^{\pm\frac{\eta_{optimum}}{10}}} \tag{4}$$

where 'n' observation number, 'η_{opt}' optimum S/N ratio, 'η_{avg}' average S/N ratio, 'η_{ideal}' ideal S/N ratio level of each control factor.

Analysis of Variance (ANOVA) and Regression Modeling

ANOVA investigates the significance of design factors on the responses and also depict their contribution on the generated responses based on F-Statistics test equations [16, 17] and the contribution is evaluated using Eq. (5) [17].

$$\%\,Contribution = MS/(MS)_{Total} \tag{5}$$

Regression second order linear models were derived based on the experimental response values of the designed DOE. It helps in predicting the behavior and effect of control factors on responses to aid the selection of working factors for a given required response. The Response (R) can be model as

$$R = K * A^a * B^b * C^c * D^d \tag{6}$$

where A, B, C and D are control factors, while K, a, b, c, d are model parameters to be estimated from experimental results.

The exponential form of responses may be converted to linear model with help of logarithmic transformation and modeled as:

$$Log(R) = \log K + a * \log(A) + b * \log(B) + c * \log(C) + d * \log(D) \tag{7}$$

The proposed second order model developed from the above functional relationship is:

$$Y = \beta_o x_o + \beta_1 x_1 + \beta_2 x_2 + \beta_4 x_3 + \beta_5 x_4 + \beta_6 x_1^2 + \beta_7 x_2^2 + \beta_8 x_3^2 + \beta_9 x_4^2 + \varepsilon \tag{8}$$

where Y is the true response on a logarithmic scale, where $x_o = 1$ (dummy variable), x_1, x_2, x_3, x_4 are logarithmic transformations of wt%, Load, Velocity and SLD respectively. β_o, β_1, β_2,…β_9 are the parameters to be estimated and ε is the experimental error.

Data Analysis and Discussions

ANOVA of SN ratios as shown in Tables 4, 5, 6, and 7 indicate that the load is highly significant with 89 % contribution in generating Avg. Sp. wear rate, while wt% and load are significant in generating friction coefficient with a minimum of 44 % contribution each.

Tables 8 and 9 show the analysis of regression models on the responses and indicates that the model depicts a significance with more than 95 % confidence level. The regression models show that load and wt% are predominant factors in predicting the Sp. wear rate and friction coefficient. The regression models were generated from the experimental results using Eq:6-8 and are as shown in Eqs: 9–10:

$$W_s = -0.5626 - 0.2517 * A + 0.0391 * B - 0.0296 * C - 2.01e - 05 * D + 0.073 * A^2 - 0.00019 * B^2 + 0.0069 * C^2 + 1.19e - 09 * D^2 \tag{9}$$

and

$$\mu = 0.0405 - 0.1442 * A + 0.0030 * B + 0.0170 * C - 1.17e - 05 * D + 0.05 * A^2 - 1.08e - 05 * B^2 - 0.0016 * C^2 + 1.91e - 09 * D^2 \tag{10}$$

Discussions on Optimality

Based on mean S/N ratios as shown in Fig. 2a, b, the optimal combinations of control factors were found as A3–B1–C3–D4 and A4–B1–C1–D2 for Sp. wear rate and friction coefficient respectively. Based on Eqs. (2)–(4) and according to the smallest is the best quality characteristic, the optimal average wear rate and frictional coefficient were determined as 0.36×10^{-6} mm^3/Nm and 0.073 respectively.

Surface plots were plotted for the first two predominant control factors on the generated responses, as shown in Fig. 3a, b. Figure 3a interprets that the wear rate tends to be decreasing effectively up to 1 wt% of reinforcement,

Table 4 Analysis of variance for Avg. sp. wear rate based on SN ratios

Source	DF	Seq SS	Adj SS	Adj MS	F	P	% Contribution
A: wt %	3	12.432	12.432	4.14	3.15	0.186	6.4
B: load	3	173.51	173.51	57.83	43.99	0.006	89.3
C: velocity	3	1.419	1.419	0.472	0.36	0.788	0.7
D: SLD	3	3.081	3.081	1.027	0.78	0.578	1.58
Residual error	3	3.945	3.945	1.314			
Total	15	194.38					

Table 5 Response table for SN ratios based on smaller-is-better

Level	Wt%	Load	Velocity	SLD
1	0.1596	7.0822	1.0635	0.9593
2	1.3387	0.6125	1.7242	1.2399
3	2.3950	−0.1597	1.8384	1.8546
4	2.1957	−1.4458	1.4629	2.0353
Delta	2.2354	8.5280	0.7749	1.0760
Rank	2	1	4	3

Table 6 Analysis of variance for friction coefficient based on SN ratios

Source	DF	Seq SS	Adj SS	Adj MS	F	P	% Contribution
A: wt%	3	68.035	68.035	22.6782	40.28	0.006	49.2
B: load	3	62.031	62.031	20.6769	36.73	0.007	44.8
C: velocity	3	1.349	1.349	0.4498	0.80	0.571	0.97
D: SLD	3	5.174	5.174	1.7247	3.06	0.191	0.03
Residual error	3	1.689	1.689	0.5630			
Total	15	138.278					

Table 7 Response table for signal to noise ratios based on smaller-is-better

Level	Wt%	Load	Velocity	SLD
1	13.68	19.78	17.12	16.86
2	16.07	17.20	16.71	17.46
3	18.63	15.33	16.32	16.84
4	18.65	14.72	16.87	15.87
Delta	4.97	5.06	0.80	1.59
Rank	2	1	4	3

Table 8 Analysis of variance for Avg. Sp. wear rate based on regression model

Source	DF	Seq SS	Adj SS	Adj MS	F	P
Regression	4	1.14156	1.14156	0.28539	16.5469	0.000127
Wt%	1	0.08712	0.08712	0.08712	5.0510	0.046097
Load	1	1.04827	1.04827	1.04827	60.7790	0.000008
Velocity	1	0.00051	0.00051	0.00051	0.0295	0.866847
SLD	1	0.00566	0.00566	0.00566	0.3283	0.578208
Error	11	0.18972	0.18972	0.01725		
Total	15	1.33128				

$S = 0.131329$, R-Sq = 85.75 %, R-Sq(adj) = 80.57 % and F-Critical (1,11) = 4.844

Table 9 Analysis of variance for friction coefficient based on regression model

Source	DF	Seq SS	Adj SS	Adj MS	F	P
Regression	4	0.0385	0.0385	0.0096	11.424	0.0006
A:wt%	1	0.0171	0.0171	0.0171	20.332	0.0007
B: load	1	0.0177	0.0177	0.0177	21.065	0.0007
C: velocity	1	0.0017	0.0017	0.0017	2.015	0.1834
D:SLD	1	0.0019	0.0019	0.0019	2.286	0.1587
Error	11	0.0092	0.0092	0.0008		
Total	15	0.0478				

S = 0.0290609, R-Sq = 80.60 %, R-Sq(adj) = 73.54 % and F-Critical (1,11) = 4.844
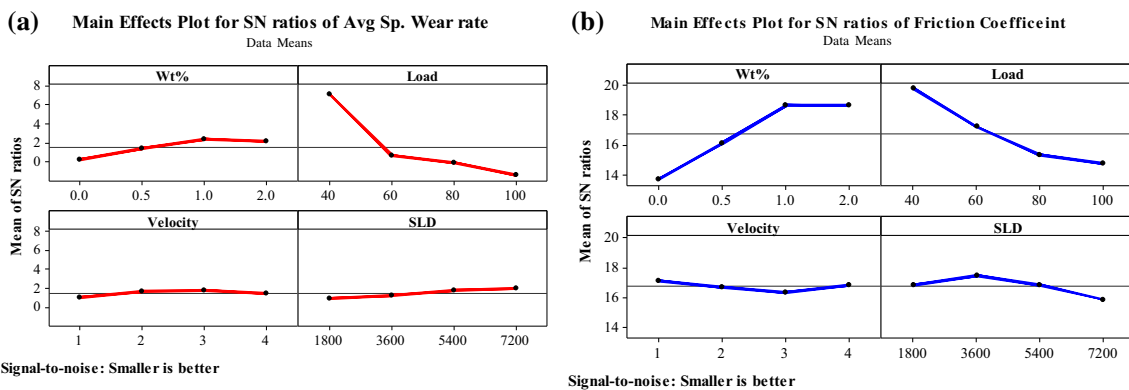
Fig. 2 Main effects of parameters on SN ratios. **a** Main effect plot for wear rate, **b** main effect plot for friction coefficient

Fig. 3 Surface plots of the responses. **a** Surface plot of wear rate against factors, **b** surface plot of friction coefficient against factors
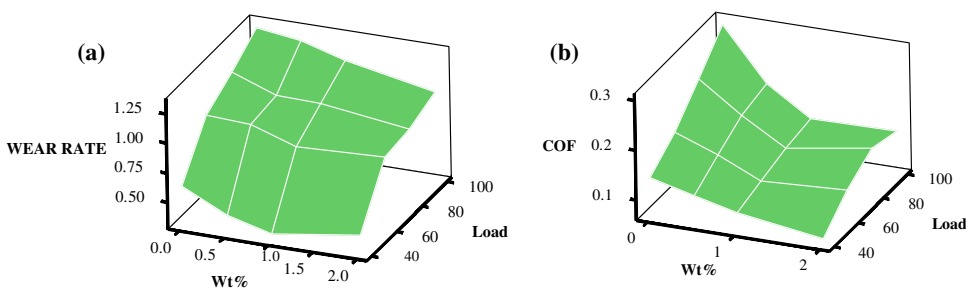
Table 10 Confirmation experiments

Response and level	Optimal control parameters	
	Predicted	Experiment
Avg. sp. wear rate (A3–B1–C3–D4)	0.36	0.33
Friction coefficient (A4–B1–C1–D2)	0.073	0.072

while Fig. 3b shows the tendency of decreasing friction coefficient throughout.

Based on the optimal control factors combinations of wear rate and friction force, the validation of experiments has been carried out and values of 'W$_s$' and 'μ' are tabulated in Table 10.

Microscopic Results

The specimens are examined under the Olympus optical microscope to determine the micro structure. Each and every specimen was cleaned with acetone, before and after the wear test to visualize the microstructures of the materials and their wear track using this optical microscope. A 5× zoom lens was used to capture image at 500 μm using computer software. Nylon66/GnP nano composites with different combination of control factors were examined on wear test rig and worn out surfaces of wear tracks were observed under microscope. Among all these combinations, the pure Nylon66 and Nylon66/GnP at 1 wt% of the tested specimens are shown in Fig. 4.
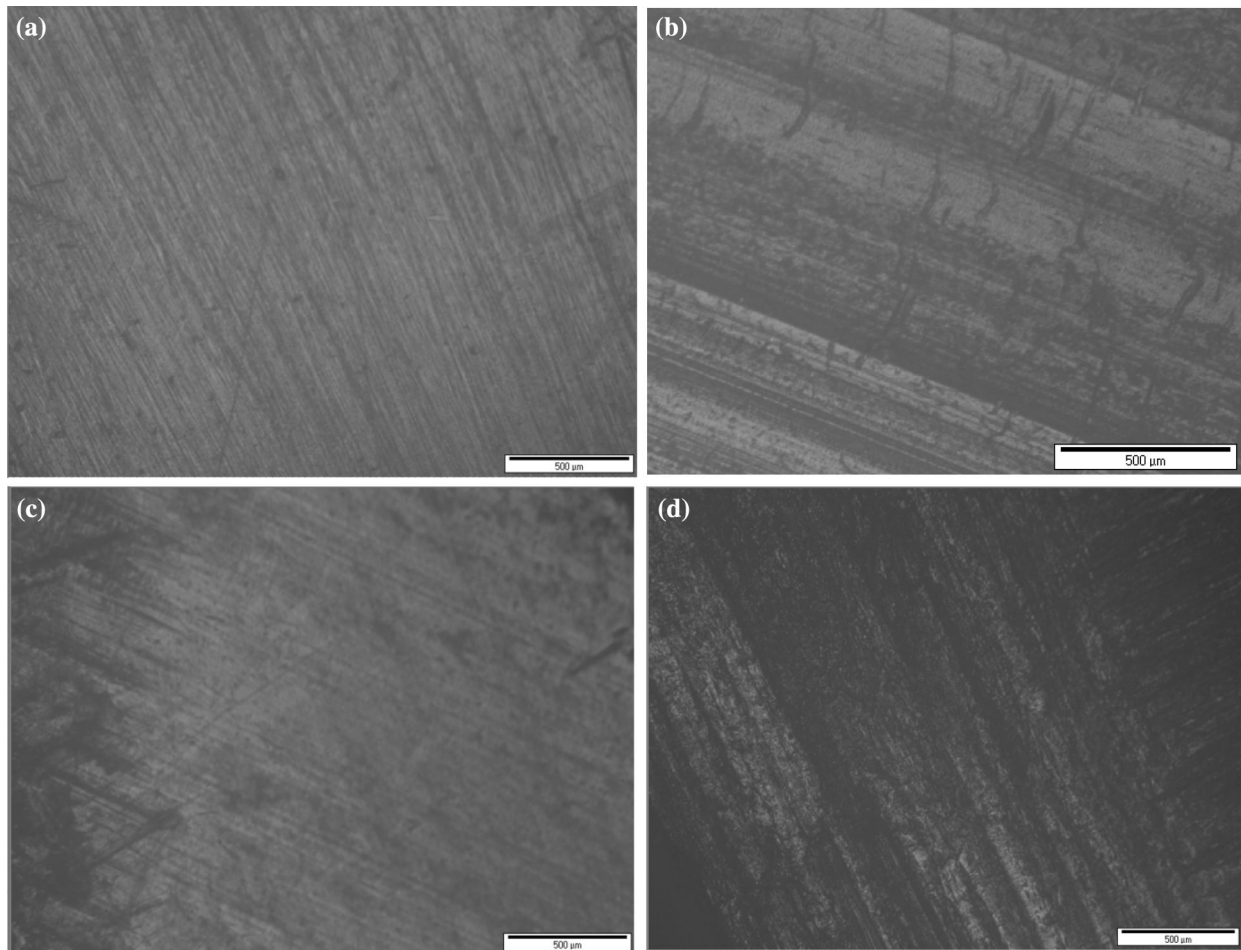
Fig. 4 Microstructures of prepared specimens before and after wear tests. **a** Nylon 66 before, wear test, **b** Nylon 66 after wear test, **c** 1 % GnP before wear test, **d** 1 % GnP after wear test

Conclusion

From DOE, the following conclusions are drawn from the present work:

1. The incorporation of the GnP particles in the polymer matrix as a reinforcement increases the wear resistance of the material.
2. From ANOVA and % contribution, effect of variables i.e., load and wt% is more predominant on the wear and friction coefficient of the composite rather than sliding velocity and sliding distance.
3. From microscopic structures, 1 wt% nylon/GnP blended specimen showing enhanced wear resistance due to less wear track widths and depths.
4. Regression modeling correlates a minimum of 80 % R^2 (goodness-of-fit) with the experimental values.
5. The confirmation test shows an error of maximum 9.09 and 1.39 % for wear rate and frictional coefficient respectively.

Compliance with Ethical Standards

Conflict of interest The authors declare that there is no conflict of interests regarding the publication of this paper.

References

1. Y.V. Suvorov, S.I. Alekseeva, M.A. Fronya, I.V. Viktorova, Investigations of physical and mechanical properties of polymeric nano composites (review). Inorg. Mater. **49**(15), 1357 (2013)
2. Z. Eliezer, C.H. Ramage, H.G. Rylander, R.H. Flowers, M.F. Amateau, High-speed tribological properties of graphite fiber-Cu-Sn matrix composites. Wear **49**(1), 119 (1978)
3. D.C. Phillips, R.A.J. Sambell, D.H. Bowen, The mechanical properties of carbon fibre reinforced pyrex glass. J. Mater. Sci. **7**, 1454 (1972)

4. R.A.J. Sambell, D.H. Bowen, D.C. Phillips, Carbon fibre composites with ceramic and glass matrices-Part1. Discontinuous fibres. J. Mater. Sci. **7**, 663 (1972)

5. S.B.C.A. Berg, J. Tirosh, Wear and friction of two different types of graphite fibre reinforced composite materials. Fibre Sci. Technol. **6**(3), 159 (1973)

6. H. Porwal, S. Grasso, M. Reece, Review of graphene-ceramic matrix composites. Adv. Appl. Ceram. **112**(8), 443 (2013)

7. H. Porwal, P. Tatarko, S. Grasso, C. Hu, A.R. Boccaccini, I. Dlouhý, M. Reece, Toughened and machinable glass matrix composites reinforced with graphene and graphene-oxide nanoplatelets. Sci. Technol. Adv. Mater. **14**, 1–10 (2013)

8. H. Porwal, S. Grasso, L. Cordero-Arias, C. Li, A. Boccaccini, M. Reece, Processing and bioactivity of 45S5 bioglasss-graphene nanoplatelets composites. J. Mater. Sci. Mater. Med. **25**(6), 1403–1413 (2014)

9. U. Khan, P. May, H. Porwal, K. Nawaz, J.N. Coleman, Improved adhesive strength and toughness of poly vinyl acetate glue on addition of small quantities of grapheme. ACS Appl. Mater. Interface **5**(4), 1423 (2013)

10. M.C. Liu, C.L. Chen, J. Hu, X.L. Wu, X.K. Wang, Synthesis of magnetite/graphene oxide composite and application for cobalt(II) removal. J. Phys. Chem. C **115**(51), 25234 (2011)

11. C. Lee, X.D. Wei, J.W. Kysar, J. Hone, Measurement of the elastic properties and intrinsic strength of monolayer grapheme. Science **321**(5887), 385 (2008)

12. A.K. Geim, K.S. Novoselov, The rise of grapheme. Nat. Mater. **6**(3), 183 (2007)

13. A.A. Balandin, Thermal properties of graphene and nano structured carbon materials. Nat. Mater. **10**(8), 569 (2011)

14. Y.C. Fan, W. Jiang, A. Kawasaki, Highly conductive few-layergraphene/Al_2O_3 nano composites with tunable charge carrier type. Adv. Funct. Mater. **22**(18), 3882 (2012)

15. P. Miranzo, E. Garcia, C. Garcia, J. Gonzalez-Julian, M. Belmonte, M.I. Osendi, Anisotropic thermal conductivity of silicon nitride ceramics. J. Eur. Ceram. Soc. **32**, 1847–1854 (2012)

16. C. Ozay, V. Savas, The optimization of Cutting parameters on surface roughness in tangential Turn-milling using Taguchi method. Adv. Nat. Appl. Sci. **6**(6), 866 (2012)

17. K. Arun Vikram, C. Ratnam, K. Sankara Narayana, B.S. Ben, Assessment of surface roughness and MRR while machining Brass with HSS tool and carbide inserts. Indian J. Eng. Mater. Sci. **22**(3), 321 (2015)

18. S.M. Phadke, *Quality Engineering using Robust Design*, vol. 59 (PTR Prentice-Hall Inc., Englewood, 1989)